PHYSICAL REVIEW B **87**, 180408(R) (2013)

Magnetoelectric hysteresis loops in Cr_2O_3 at room temperature

Ayato Iyama and Tsuyoshi Kimura

Division of Materials Physics, Graduate School of Engineering Science, Osaka University, Toyonaka, Osaka 560-8531, Japan

(Received 22 April 2013; revised manuscript received 6 May 2013; published 28 May 2013)

We revisit the room-temperature linear magnetoelectric effect in Cr_2O_3 single crystals. It was found that the temperature dependence of dielectric constants in a magnetic field H shows a λ-shaped peak at the Néel temperature (≈307 K) and that electric polarization induced by applying H is reversed with a hysteresis by sweeping an electric field E. Similar reversal and hysteretic behaviors were also observed in the H dependence of magnetization induced by applying E. These results imply that Cr_2O_3 behaves as a typical ferroelectric (ferromagnet) in finite H (E) even at room temperature. We discuss the ferroic behaviors observed in the linear magnetoelectric system in the context of recent studies on multiferroics.

DOI: 10.1103/PhysRevB.87.180408 PACS number(s): 75.85.+t, 75.47.Lx, 75.60.−d

The linear magnetoelectric (ME) effect, in which electric polarization P (magnetization M) is induced in proportion to an applied magnetic field H (electric field E), was first observed in Cr_2O_3 a half century ago[1–3] and is expressed by $P_i = \alpha_{ij} H_j$ or $M_i = \alpha_{ij} E_j$.[4,5] Whether the proportionality coefficient α_{ij} (termed the ME tensor) is finite or zero is determined by the phenomenological symmetry requirement.[6] As a consequence, the linear ME effect is allowed only in materials in which both space-inversion and time-reversal symmetries are broken. Since the first observation of the linear ME effect,[2] Cr_2O_3 has long been attracting attention in terms of its ME[7–9] and related magneto-optical properties such as second harmonic generations[10] and nonreciprocal optical rotation.[11] Cr_2O_3 has a corundum structure with the space group $R\bar{3}c$ and shows an antiferromagnetic (AFM) order below $T_N \approx 307$ K[12] [see the inset of Fig. 1(a)]. This AFM ordering makes its magnetic symmetry $\bar{3}'m'$, breaks both the space-inversion and time-reversal symmetries, and then allows the diagonal linear ME effect in which α_{ij} $(i = j)$ can be finite.[1] To explain the linear ME effect microscopically, several models were proposed in the early stage of ME research.[13–16] Furthermore, recent extensive studies on multiferroics have brought renewed attention to the understanding of the linear ME effect in Cr_2O_3. Lately, several groups tackled this classical problem by utilizing modern theoretical techniques such as the first-principles calculations.[17–21] These recent theoretical studies discussed the spin-lattice, spin-electronic, and orbital contributions to the linear ME effect. However, the origin is still under debate.

Moreover, Cr_2O_3 with $T_N \approx 307$ K is not only the first ME compound but also a rare example showing the ME effect at *room temperature*. In spite of recent extensive research activities on multiferroics, room-temperature ME operation has been achieved only in a few systems (e.g., $Sr_3Co_2Fe_{24}O_{41}$).[22] This rare characteristic, that is, room-temperature ME operation, has driven recent research on Cr_2O_3 for future applications.[23,24] However, detailed experimental data of ME properties in the vicinity of T_N have been lacking (e.g., the temperature dependence of dielectric constants around the phase boundary). Besides, it is beneficial to discuss the linear ME effect from the viewpoint of multiferroics, which can promote the understanding of the two relevant phenomena. In this Rapid Communication, we provide various experimental results on magnetoelectric properties, i.e., E-induced M and H-induced P, in Cr_2O_3 around room temperature, and demonstrate that the linear ME system exhibits ferroic natures, i.e., phase transition and domain switching in its electric and magnetic properties in the presence of applied H and E, respectively.

Single crystals of Cr_2O_3 were grown from Bi_2O_3 flux in a similar way to that described in Ref. 25. The obtained crystals were in plate shapes ($\sim 2 \times 1 \times 0.1$ mm^3) with the largest faces perpendicular to the c axis (hexagonal setting). Silver electrodes were vacuum deposited onto the largest faces for measurements of dielectric constant along c (ε_c), electric polarization along c (P_c), and magnetization along c (M_c). An *LCR* meter, an electrometer, and a vibrating sample magnetometer were used for the measurements of ε_c, P_c, and M_c, respectively. To measure M_c, a homemade insert which allows the application of E was installed in the magnetometer. The respective measurements of P_c and M_c were carried out after cooling the samples from a temperature above T_N in the presence of both E and H (ME-field-cooling procedure). In Cr_2O_3 with the magnetic symmetry $\bar{3}'m'$, the ME tensor components α_{11} $(=\alpha_{22})$ and α_{33} can be finite. In this study, however, H and E were applied only along the c axis during the ME field cooling and the measurements, which means that only α_{33} was investigated.

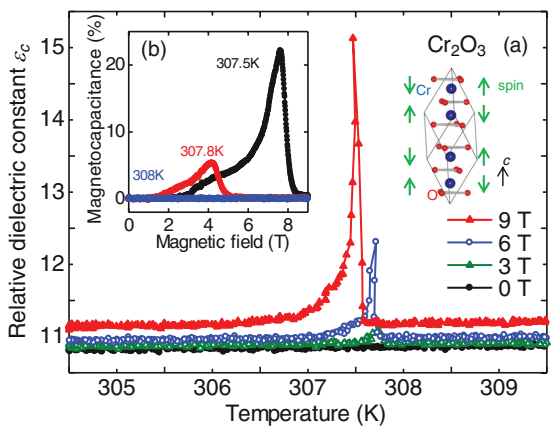

FIG. 1. (Color online) The relative dielectric constant along c as functions of (a) temperature and (b) magnetic field applied along c. Schematic crystal and magnetic structures are shown in the inset.

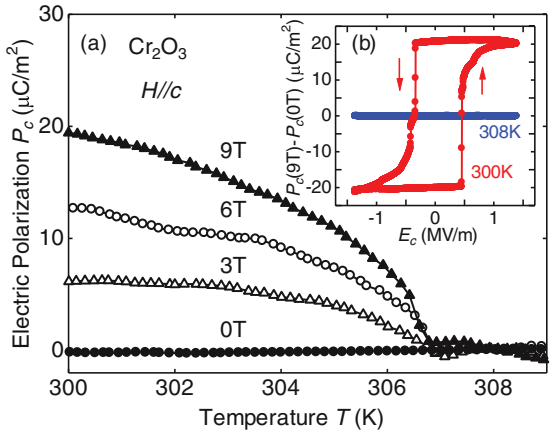

FIG. 2. (Color online) (a) Temperature dependence of the electric polarization along c in selected magnetic fields applied along c. (b) The difference of the electric polarization measured at 9 T and 0 T as a function of the electric field. The data of (b) were taken at 300 and 308 K.

Figure 1(a) shows the temperature (T) dependence of ε_c measured at 1 kHz in the vicinity of T_N. At $\mu_0 H = 0$ T (where μ_0 is the magnetic permeability of vacuum), ε_c is almost T independent in this T range, and the absolute value ($\varepsilon_c \approx 11$) is consistent with that in previous results.[26,27] However, by applying H, ε_c shows a λ-shaped peak at T_N. The λ-shaped anomaly in the T profiles of ε_c is reminiscent of a second order ferroelectric phase transition. This anomaly is not observed without an applied H, meaning that it is relevant to H-induced P through the linear ME effect. With increasing H, the peak feature becomes more pronounced, and the peak position shifts towards lower T in accordance with a decrease of T_N in higher H. The H-dependent ε_c gives rise to a distinct magnetocapacitance, as shown in Fig. 1(b). This magnetocapacitive effect is prominent around a phase boundary between paramagnetic and antiferromagnetic ME states, and represents the fluctuation of P_c induced by H in the vicinity of the transition point. The magnetocapacitance defined as $[\varepsilon_c(H) - \varepsilon_c(0)]/\varepsilon_c(0)$ exceeds 20% at $T = 307.5$ K and $\mu_0 H \approx 7.5$ T.

Figure 2(a) shows T dependence of P_c in selected magnetic fields. Although no net P_c was observed at 0 T in all the T range, P_c develops below T_N by applying H. The T dependence of P_c is reminiscent of that of the staggered magnetization G_c obtained by a neutron scattering measurement.[28] This suggests that an order parameter of the in-field ferroelectricity originates from G_c, which is consistent with Ref. 18 because the magnetic susceptibility along c (χ_c) is almost constant in this T range. The induced P_c is nearly proportional to an applied H. Thus, the H-induced P_c below T_N (Fig. 2) as well as the dielectric anomaly around T_N (Fig. 1) is ascribed to the linear ME effect. From the H dependence of P_c at 300 K, we obtained $\alpha_{33} = 2.8$ ps/m, which is comparable to the latest previous result (see Ref. 9 in which α_{33} is 2.7 ps/m at 300 K). Figure 2(b) shows the E dependence of P_c(9 T)–P_c(0 T). No change in P_c(9 T)–P_c(0 T) was observed at 308 K ($>T_N$), while that at 300 K ($<T_N$) is reversed

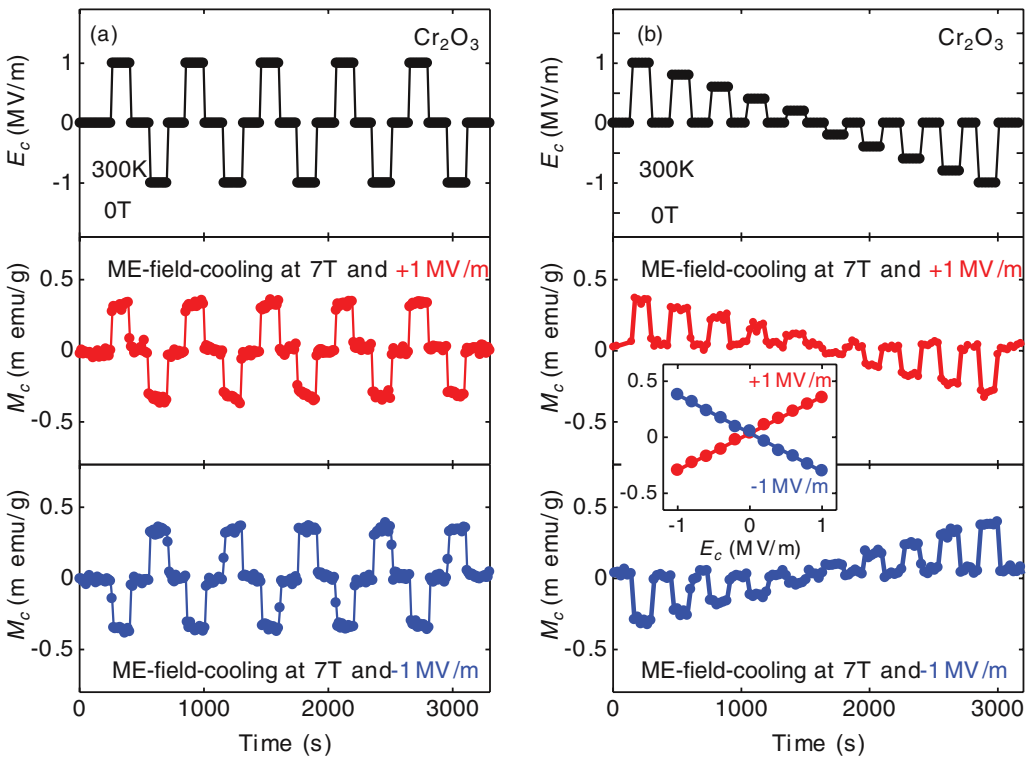

FIG. 3. (Color online) Temporal evolution of magnetization along c (M_c) responding to periodically applied electric fields along c (E_c) at $T = 300$ K and $\mu_0 H = 0$ T. Top panels of (a) and (b) show applied E_c as a function of time. Middle and bottom panels display the corresponding M_c data. Prior to the measurements of the middle and bottom panels, the ME field cooling was done at $\mu_0 H_c = 7$ T with $E = 1$ MV/m and -1 MV/m, respectively. The inset of (b) shows M_c as a function of E_c and represents the linear relationships between M_c and applied E_c.

with a hysteresis by sweeping E. The result demonstrates that Cr_2O_3 shows a typical ferroelectric behavior at room temperature in the presence of H. This ferroelectric behavior, i.e., the E reversal of P_c, is ascribed to a switching of the antiferromagnetic domains[29,30] because a change in the sign of G_c leads to a sign reversal of P_c.[18]

Next, we investigated the inverse ME effect, that is, the effect of E on M, around room temperature. Figure 3(a) shows our experimental demonstration of the E-induced magnetization reversal without altering H at 300 K. Prior to the measurement shown in the middle panel of Fig. 3(a), the sample was cooled at $E_c = 1$ MV/m and $\mu_0 H_c = 7$ T from a temperature above T_N (ME field cooling). After the sample was set at 300 K, both E and H were removed. Subsequently, $E_c = 0, +1$, and -1 MV/m were applied periodically [top panel of Fig. 3(a)]. As seen in the middle panel of Fig. 3(a), M_c is induced by applying E. In addition, as the sign of E is reversed, E-induced M_c is also reversed. When the ME field cooling was done, $E_c = -1$ MV/m and $\mu_0 H = 7$ T, the sign of the E-induced M_c is reversed [compare the middle and bottom panels of Fig. 3(a)].

Furthermore, the magnitude of E-induced M_c linearly depends on the applied E. Figure 3(b) displays temporal evolution of M_c (middle and bottom panels) responding to various applied E (top panel) at $T = 300$ K in $\mu_0 H = 0$ T. Prior to the measurements, the sample was cooled at $E_c = +1$ MV/m (middle panel) or -1 MV/m (bottom panel) in $\mu_0 H_c = 7$ T. As evidently seen in the inset of Fig. 3(b), the E-induced M_c is proportional to the applied E. These results originate from the inverse linear ME effect. Indeed, the ME tensor estimated from dM_c/dE is $\alpha_{33} = 2.9$ ps/m, which is equivalent to the value obtained from an independent measurement of H-induced P. These experimental results clearly demonstrate that the sign and the magnitude of M can be finely controlled only by applying E in Cr_2O_3 at room temperature.

In the inset of Fig. 2, we presented a P-E hysteresis curve, i.e., a ferroelectric characteristic, in the presence of H. Since the ME tensor is totally symmetric between electric and magnetic properties, ferromagnetic behaviors can also be expected in E. Figure 4(a) represents the T dependence of M_c in selected E_c after ME field cooling at 7 T and the selected E_c. Although M_c is zero without E_c, M_c arises below T_N in E_c similarly with the P_c-T curve shown in Fig. 2. The E-induced M_c is reversed by applying the opposite E_c after the same ME-field-cooling procedure as seen in Fig. 4(b). Figure 4(f) shows the difference of M_c at 2.3 MV/m and M_c at 0 MV/m [$\Delta M_c(2.3\ \mathrm{MV/m}) = M_c(2.3\ \mathrm{MV/m}) - M_c(0\ \mathrm{MV/m})$] as a function of applied H. The measurement protocol is as follows. First, we cooled the sample at both $E = 2.3$ MV/m and $\mu_0 H = 1$ T to 290 or 308 K from ~320 K. Second, M_c was measured with applying E as a function of time. After 2 min, E was turned off, and subsequently M_c was measured for the following 2 min [Fig. 4(c)]. Then, we obtained the average and the standard deviation of $\Delta M_c(2.3$ MV/m) at a selected H. Next, we turned on E, and changed H to the next point. This procedure was repeated with changing H to various values ($-7\ \mathrm{T} \leqslant H \leqslant 7$ T). As examples, the experimental data obtained at -2 and -6 T during H sweeping to -7 T are shown in Figs. 4(d) and 4(e), respectively. In this way, we obtained $\Delta M_c(2.3$ MV/m) $-$ H curves at 290 and 308 K.

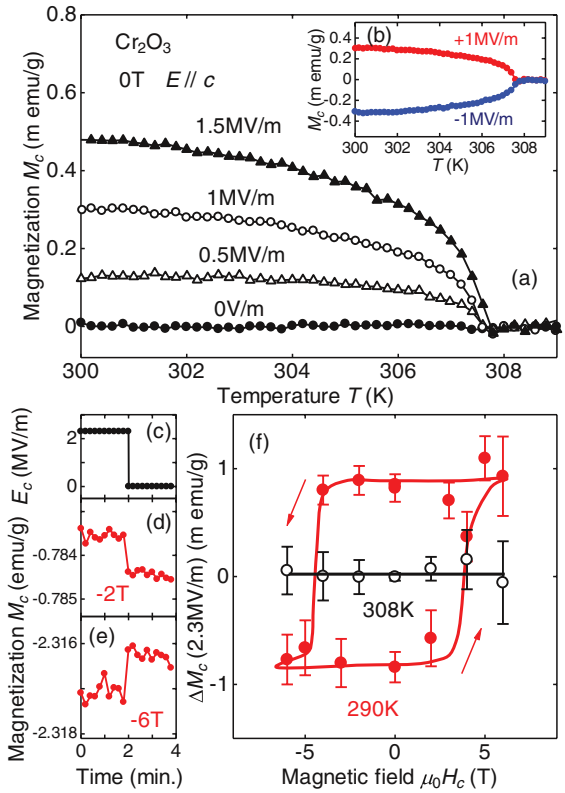

FIG. 4. (Color online) Temperature dependence of the magnetization along c in (a) selected electric fields and in (b) the opposite electric fields applied along c. Time dependence of (c) the applied electric field and the magnetization in (d) -2 T and (e) -6 T at 290 K. First, we applied an electric field for 2 min during the measurement. After that, we turned off the electric field, and measured magnetization for the following 2 min. (f) The difference of the magnetization measured at 2.3 MV/m and 0 V/m as a function of the magnetic field. Black open and red solid circles denote the data obtained at 308 and 290 K, respectively.

At 308 K ($>T_N$), no substantial change in $\Delta M_c(2.3$ MV/m) was observed in all the H [black open circles in Fig. 4(f)]. In contrast, a clear hysteresis loop was observed at 290 K [red solid circles in Fig. 4(f)]. Namely, E-induced M_c is reversed with a hysteresis by sweeping H at 290 K. This result demonstrates that Cr_2O_3 behaves as a ferromagnet with a large coercive field (~4.5 T) in the presence of $E = 2.3$ MV/m at room temperature.

From our experimental results, it is obvious that Cr_2O_3 shows ferroelectric behaviors in H and ferromagnetic behaviors in E at room temperature. First, we discuss its ferroelectric nature in H in the context of that in spin-driven ferroelectrics in which the appearance of ferroelectricity is ascribed to the development of an order parameter arising from a complex magnetic ordering. For example, the order parameter in one of the most famous spin-driven ferroelectrics, $TbMnO_3$, is the so-called vector spin chirality which resides in a noncollinear spiral spin ordered state.[31] Thus, in spin-driven ferroelectrics, their order parameters inside the systems make them polar. On the other hand, the ME effect in Cr_2O_3 has been explained by a recent phenomenological theory[18] in which the H-induced P along c is expressed as $P_c\ (=\alpha_{33} H_c) \propto \lambda \chi_c G_c H_c$. Here λ is

the coupling strength. Following this model, the combination of the staggered magnetization G_c (order parameter inside the system) and the applied magnetic field H_c (external field) make the system polar in Cr_2O_3. Based on the symmetry argument, this is the only difference between spin-driven ferroelectrics and the linear ME Cr_2O_3. As a consequence, in H, Cr_2O_3 shows similar ferroelectric behaviors with spin-driven ferroelectrics such as $TbMnO_3$ (pseudoproper ferroelectricity in this case[32]). This is probably because H corresponds to the frozen order parameter S_3 which has been already activated at high temperature, and G_c corresponds to the order parameter S_2 at the multiferroic phase transition described in Ref. 32, which explains that ferroelectric P in $TbMnO_3$ is proportional to the order parameters S_2S_3. Indeed, ε and P in H of Cr_2O_3 behave in a similar way with those of $TbMnO_3$. In this manner, the linear ME effect (and the behavior of ε around the phase transition) is naturally understood.

Next, we briefly discuss what induces a hysteresis in the same context. In $TbMnO_3$, the sign of vector spin chirality determines the sign of ferroelectric polarization. On the other hand, in Cr_2O_3, the signs of G_c and H_c determine the sign of P_c. In the P-E hysteresis measurement (Fig. 2), we applied H and swept E. When the H-induced P is reversed, it should be accompanied by a reversal of G_c, as mentioned above, because we fixed H during the measurement. Therefore, the reversal of G_c induces a hysteresis, and this situation is the same in an M-H hysteresis measurement. This is, in fact, consistent with previous studies[29,30] because ME domains are identical with antiferromagnetic domains in Cr_2O_3.

To summarize, we revisited the classical linear ME effect in Cr_2O_3 by measuring magnetocapacitance, electric polarization (P) induced by a magnetic field (H), and magnetization (M) induced by an electric field (E) at room temperature. Our experimental results revealed that the first ME compound Cr_2O_3 shows ferromagnetic and ferroelectric behaviors in E and H, respectively, by properly confirming a λ-type anomaly in the dielectric constant at the Néel temperature and hysteresis loops in M-H and P-E curves. Furthermore, we experimentally demonstrated M switching only by E at room temperature. The observed in-field ferroic natures in the linear ME compound are similar to those in some multiferroics such as spin-driven ferroelectrics, and can provide an appropriate contribution to a comprehensive understanding of the classical linear ME effect and recent studies on multiferroics.

We thank Y. Yamaguchi for his help in experiments. This work was supported by KAKENHI (Grant No. 24244058) and the Global COE Program (Program No. G10), MEXT, Japan.

[1] I. E. Dzyaloshinskii, Zh. Exp. Teor. Fiz. **33**, 881 (1959) [Sov. Phys. JETP **10**, 628 (1960)].
[2] D. N. Astrov, Sov. Phys. JETP **11**, 708 (1960).
[3] G. T. Rado and V. J. Folen, Phys. Rev. Lett. **7**, 310 (1961).
[4] M. Fiebig, J. Phys. D: Appl. Phys. **38**, R123 (2005).
[5] T. H. O'Dell, *The Electrodynamics of Magneto-Electric Media* (North-Holland, Amsterdam, 1970).
[6] R. R. Birss, *Symmetry and Magnetism* (North-Holland, Amsterdam, 1964).
[7] E. Kita, A. Tasaki, and K. Siratori, Jpn. J. Appl. Phys. **18**, 1361 (1979).
[8] Y. F. Popov, A. M. Kadomtseva, D. V. Belov, G. P. Vorob'ev, and A. K. Zvezdin, JETP Lett. **69**, 330 (1999).
[9] P. Borisov, A. Hochstrat, V. V. Shvartsman, and W. Kleemann, Rev. Sci. Instrum. **78**, 106105 (2007).
[10] M. Fiebig, D. Fröhlich, B. B. Krichevtsov, and R. V. Pisarev, Phys. Rev. Lett. **73**, 2127 (1994).
[11] B. B. Krichevtsov, V. V. Pavlov, R. V. Pisarev, and V. N. Gridnev, Phys. Rev. Lett. **76**, 4628 (1996).
[12] T. R. McGuire, E. J. Scott, and F. H. Grannis, Phys. Rev. **102**, 1000 (1956).
[13] G. T. Rado, Phys. Rev. Lett. **6**, 609 (1961).
[14] M. Date, J. Kanamori, and M. Tachiki, J. Phys. Soc. Jpn. **16**, 2589 (1961).
[15] S. Alexander and S. Shtrikman, Solid State Commun. **4**, 115 (1966).
[16] R. Hornreich and S. Shtrikman, Phys. Rev. **161**, 506 (1967).
[17] J. Íñiguez, Phys. Rev. Lett. **101**, 117201 (2008).
[18] M. Mostovoy, A. Scaramucci, N. A. Spaldin, and K. T. Delaney, Phys. Rev. Lett. **105**, 087202 (2010).
[19] E. Bousquet, N. A. Spaldin, and K. T. Delaney, Phys. Rev. Lett. **106**, 107202 (2011).
[20] A. Malashevich, S. Coh, I. Souza, and D. Vanderbilt, Phys. Rev. B **86**, 094430 (2012).
[21] A. Scaramucci, E. Bousquet, M. Fechner, M. Mostovoy, and N. A. Spaldin, Phys. Rev. Lett. **109**, 197203 (2012).
[22] Y. Kitagawa, Y. Hiraoka, T. Honda, T. Ishikura, H. Nakamura, and T. Kimura, Nat. Mater. **9**, 797 (2010).
[23] P. Borisov, A. Hochstrat, X. Chen, W. Kleemann, and C. Binek, Phys. Rev. Lett. **94**, 117203 (2005).
[24] X. He, Y. Wang, N. Wu, A. N. Caruso, E. Vescovo, K. D. Belashchenko, P. A. Dowben, and C. Binek, Nat. Mater. **9**, 579 (2010).
[25] G. Garton, S. H. Smith, and B. M. Wanklyn, J. Cryst. Growth **13-14**, 588 (1972).
[26] P. H. Fang and W. S. Brower, Phys. Rev. **129**, 1561 (1963).
[27] H. B. Lal, R. Srivastava, and K. G. Srivastava, Phys. Rev. **154**, 505 (1967).
[28] E. J. Samuelsen, M. T. Hutchings, and G. Shirane, Physica **48**, 13 (1970).
[29] T. J. Martin and J. C. Anderson, IEEE Trans. Magn. **2**, 446 (1966).
[30] C. A. Brown and T. H. O'Dell, IEEE Trans. Magn. **5**, 964 (1969).
[31] S.-W. Cheong and M. Mostovoy, Nat. Mater. **6**, 13 (2007).
[32] P. Tolédano, Phys. Rev. B **79**, 094416 (2009).